metals

MDPI

Article

Pulsed Magnetic Treatment of Cobalt for Enhanced Microstructures and Mechanical Properties

Yajie Li [1], Han Guo [2], Lin Zhang [1], Zhe Chen [1], Lanhui Liu [3] and Jian Liu [1,*]

[1] School of Mechanical Engineering, Sichuan University, Chengdu 610065, China
[2] School of Aerospace, Mechanical and Mechatronic Engineering, University of Sydney, Sydney, NSW 2006, Australia
[3] National Engineering Laboratory for Industrial Big-Data Application Technology, Chongqing Innovation Center of Industrial Big-Data Co., Ltd., Chongqing 400707, China
* Correspondence: liujian@scu.edu.cn

Abstract: In this study, the effects of pulsed magnetic treatment (PMT) on the microstructure and performance of pure bulk cobalt (Co) were investigated to reveal the underlying influencing mechanism of the pulsed magnetic field on ferromagnetic materials. The hardness of the material could be increased by PMT, with a maximum increase of 3.16% when 1T was adopted. The imposition of the pulsed field promoted the transformation of Co from face-centered cubic (FCC) phase to hexagonal close-packed (HCP) phase, which obeys the Shoji–Nishiyama orientation rule, with a decrease of α-Co by 8.60% and an increase of ε-Co by 0.19%. PMT also caused multiplication of defects and the formation of low-angle grain boundaries within the bulk Co. PMT could be an effective way to modify materials to suit engineering applications.

Keywords: cobalt; electron backscattering diffraction; dislocation; phase transformations; hardness

check for updates

Citation: Li, Y.; Guo, H.; Zhang, L.; Chen, Z.; Liu, L.; Liu, J. Pulsed Magnetic Treatment of Cobalt for Enhanced Microstructures and Mechanical Properties. *Metals* **2022**, *12*, 1775. https://doi.org/10.3390/met12111775

Academic Editor: Andreas Chrysanthou

Received: 12 September 2022
Accepted: 10 October 2022
Published: 22 October 2022

Publisher's Note: MDPI stays neutral with regard to jurisdictional claims in published maps and institutional affiliations.

Copyright: © 2022 by the authors. Licensee MDPI, Basel, Switzerland. This article is an open access article distributed under the terms and conditions of the Creative Commons Attribution (CC BY) license (https://creativecommons.org/licenses/by/4.0/).

1. Introduction

Cobalt (Co), a lustrous gray-silver metal with ferromagnetic properties, has been widely used as an important element in the production of cemented carbides, super-alloys, magnetic alloys, etc. due to its exceptional mechanical and functional properties [1,2]. Two crystal types of Co phase are present in alloys. One is the low-temperature phase of hexagonal close-packed (HCP) ε-Co and the other is the high-temperature phase of face-centered-cubic (FCC) α-Co. Phase transition between these two structures usually occurs at 427 °C during slow heating and cooling processes [3]. In particular, the α-Co phase has 12 sliding surfaces with excellent toughness while the ε-Co phase has 3 sliding surfaces with lower toughness and better wear resistance [4]. At room temperature, a Co phase generally presents as ε-Co with a small amount of α-Co; the Co phase is usually used as a binder in the preparation of alloys for their plasticity and toughness [5], can absorb energy and effectively alleviate crack propagation [6].

In recent years, there is an emerging environmentally friendly post-processing treatment using pulsed magnetic field to improve the performance of metallic materials. This pulsed magnetic treatment (PMT) bears the advantages of a shorter processing time and a lower processing temperature compared to traditional heat treatment. Quan et al. [7] found that PMT could provide a more uniform residual stress distribution on the surface of materials to enhance fatigue life [8]. Fei et al. [9] found that PMT could enhance the tribological properties of a metal alloy. Ma et al. [10] revealed that multiplication and motion of dislocation could be induced by the pulsed field to improve the micro-hardness of high-speed steel. Tang et al. [11] and Li et al. [12] indicated that the substructure of dislocations and phase transformations in titanium alloys could also be changed under a pulsed magnetic field. Although there are many reports on the processing of various metallic materials using PMT, there are scarce investigations on pure Co, an important

phase in cemented carbide tools. In a previous study by the author [13], it was proven that a pulsed magnetic field could enhance the mechanical performance of a WC/Co alloys, and this enhancement was mainly attributed to the increased dislocation density; nonetheless, the effects of the pulsed field on the Co remained unclear. As a ferromagnetic element, Co is expected to be easily affected by PMT. The aim of this study is to investigate the effects of PMT on the microstructure and properties of pure Co, and the obtained results are expected to provide a theoretical basis for the strengthening mechanism in alloys with Co induced by a pulsed magnetic field.

2. Materials and Methods

The bulk Co samples (ZhongNuo Advanced Material (Beijing) Technology Co., Ltd., Beijing, China), which were cylinders with a diameter of 3 mm and a height of 3 mm, featured a purity of 99.98%. PMT parameters with intensities from 0 to 1.5 T and pulse periods of 30 s were adopted to treat the Co samples. Figure 1 shows the schematic diagram of the magnetic field used for the treatment process and the distribution of the magnetic field near the samples. The pulsed magnetic field with a specific waveform is introduced by adjusting the coil current. The magnetic induction line passes through the sample, causing microscopic phase changes inside the sample.

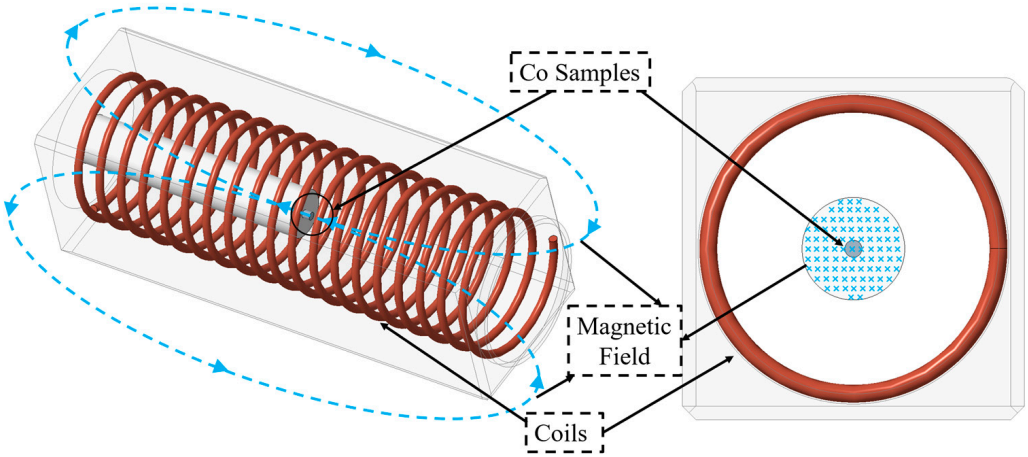


Figure 1. Principle of action of pulsed magnetic field treatment.

After the treatment, Vicker hardness was evaluated using a tester (FUTURE FM-ARS9000, Kawasaki, Japan) under a 30 kg load for 15 s on the bulk sample. A total of three rounds of hardness experiments were carried out on the samples, and the surface of each sample was evenly divided into three parts. In each round of the hardness experiments, the hardness data of these three different areas of each sample were collected. Phase compositions of the specimens were performed with an X-ray diffractometer (XRD) (EMPYREAN, PANalytical B.V., Almelo, the Netherlands) using a Co-Kα X-ray beam generator with a scanning rate of 0.06 °C/s and a scan range of 20–110 °C. Phase transformation, misorientations and defects were detected by electron backscattered diffraction (EBSD) (FEI Quanta 650F, FEI Company, Hillsboro, OR, USA) with a step size of 0.2 µm. Defects within Co were characterized via TEM (FEI Tecnai G2 F20, FEI Company, Hillsboro, OR, USA).

3. Results and Discussions

3.1. XRD Pattern and Hardness Change

XRD patterns of the Co phase before and after the treatment are shown in Figure 2a, which confirms that ε-Co phase with the HCP structure was the main phase in bulk Co at room temperature while α-Co phase with the FCC structure was a minor fraction. Figure 2b shows the hardness under different PMT strengths. It can be observed that the hardness of all the samples showed slight improvements compared to the untreated (UT) sample,

and particularly the maximum increase of approximately 3.16% was achieved when 1T treatment was used.

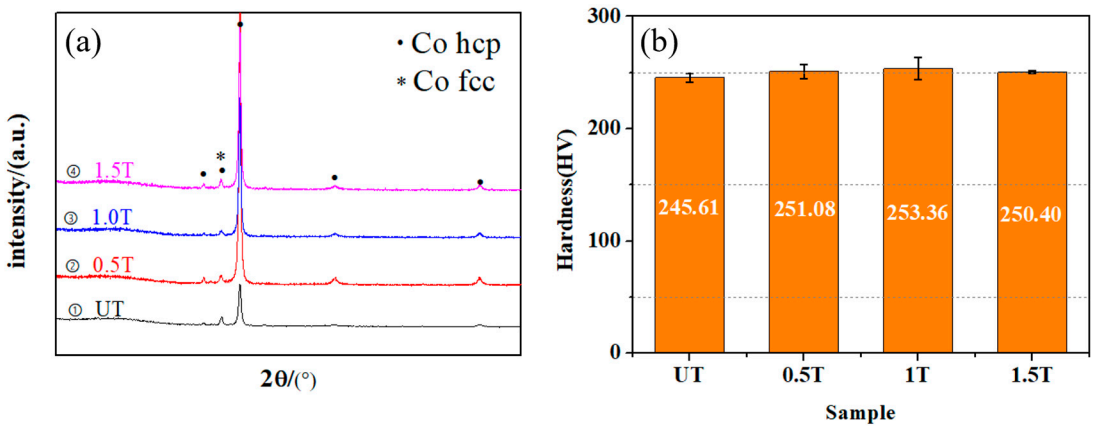


Figure 2. XRD (**a**) and hardness (**b**) of samples after PMT using the 0–1.5T processing parameters.

3.2. Phase Transition and Misorientation

EBSD characterization was conducted by comparing the 1T-treated and the untreated samples to reveal the effects of PMT on the microstructure of Co. Figure 3 shows the phase distribution of Co before and after treatment as obtained by the in situ EBSD, and the contents of the two phases are quantified in Table 1. In the figure, the red represents α-Co (FCC) and the blue indicates ε-Co (HCP). It can be observed that the percentage of α-Co decreased by 8.6% while that of the ε-Co increased by 0.19% after the PMT, which suggests the phase transformation from α-Co to ε-Co occurred with the imposition of the pulsed magnetic field. Huang et al. [14] elucidated that when the externally supplied energy reached the enthalpy of allotropic transformation of Co, phase transitions would take place and could be promoted by the accumulation of defects caused by the applied energy. Therefore, it is expected that the imposed pulsed field tends to impart energy within the Co and facilitate the formation of defects to enhance the phase transformation. Meanwhile, it is noted that texture evolution occurred with the phase transformation process, as indicated by red circles in Figure 3c,d. A strong pole was formed in the <001> and <101> directions in the FCC phase along Y_0 and Z_0 while there was hardly any change in HCP (Figure 3e,f). The difference in the crystal orientation in FCC and HCP is clear evidence that the pulsed field tended to agitate the FCC phase to initiate the phase transformation from the FCC to HCP phase. As is known, the α-Co has the lattice coefficient of $a = b = c = 0.3545$ nm while ε-Co has the lattice coefficients of $a = b = 0.2503$ nm and $c = 0.4061$ nm. A single Co atom in the FCC phase occupies a volume of 0.011138 nm^3, while one in HCP has a unit cell volume of 0.011079 nm^3. Therefore, there will be strain energy during the phase transformation of Co, and to reduce interface energy between the FCC and HCP phases, defects such as dislocations, stacking faults, and low-angle grain boundaries are expected to be formed simultaneously. As a result, the Co will be strengthened, and a relatively high hardness will be achieved due to the defects induced by the pulsed magnetic field.

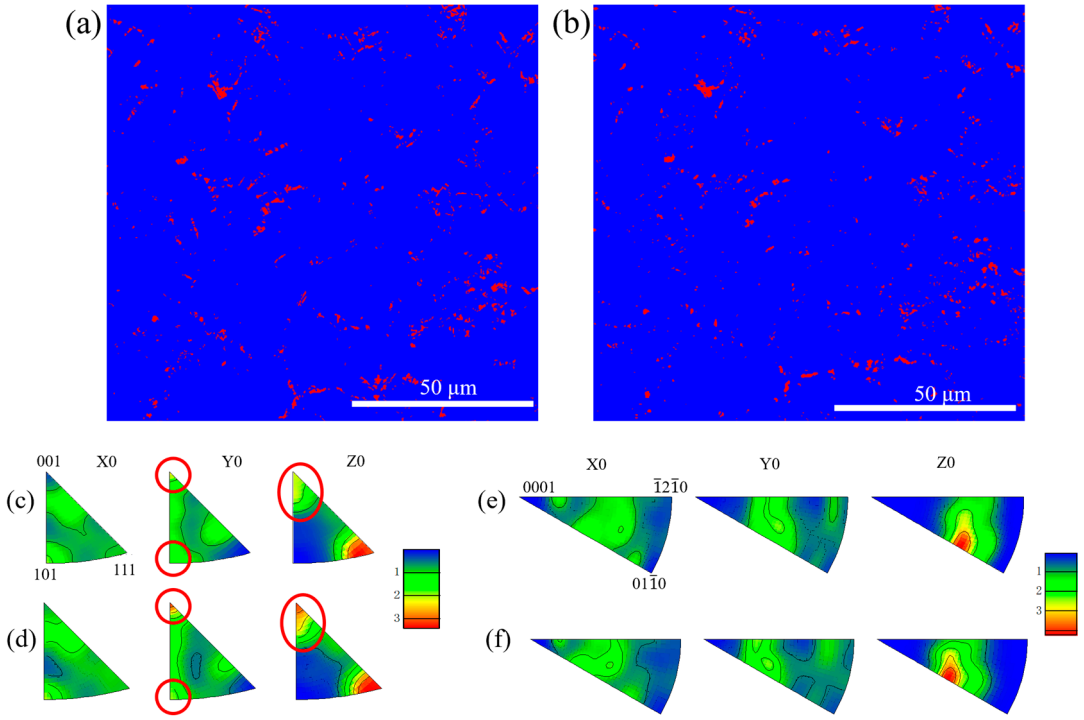


Figure 3. Distribution of two phases in bulk Co sample and pole figure of the FCC and HCP phases. Red: FCC; blue: HCP. (**a**,**c**,**e**) UT; (**b**,**d**,**f**) 1T.

Table 1. Content of phase of bulk Co sample before and after the PMT.

Phase	UT	1T
HCP (ε-Co)	97.79%	97.98%
FCC (α-Co)	2.21%	2.02%

The surface of the bulk Co was investigated using the X direction (Y-Z plane) of the EBSD, and the inverse pole figures (IPFs) from the EBSD are shown in Figure 4a–d. It can be observed that the bulk Co sample showed grain orientation changes in both the FCC and HCP phases after the treatment, with an increase in the percentage of low-angle grain boundaries (LAGBs, 2–15°), as indicated by the additional colored dots in the highlighted circles in the figure. Grain boundary misorientations and the relative frequency of the phase are provided in Figure 4e,f for further analysis. In the figure, LAGBs are denoted by the red line, and high-angle grain boundaries (HAGBs, >15°) are denoted by the black line. It is clear that the amount of LAGBs increased significantly in Figure 4f after the treatment, and statistical results of the frequency distribution of misorientation in the grains (Figure 4e1–f2) revealed that the formation of LAGBs was promoted with the imposition of the pulsed field, accompanying a decreasing amount of HAGBs. It is suggested that LAGBs are lattice defects formed by multiple dislocation networks [15] and are usually formed when dislocations change from a higher energy level of pile-up to a lower-energy dislocation wall in the direction perpendicular to the slip plane. It is also expected that the original grains may be split into many sub-grains with slightly different orientations [16] after the treatment, and the newly formed sub-grains, presented as red dots in Figure 4f, increase the density of the boundaries [17], which would strengthen the materials along with defects formed during the pulsed field treatment.

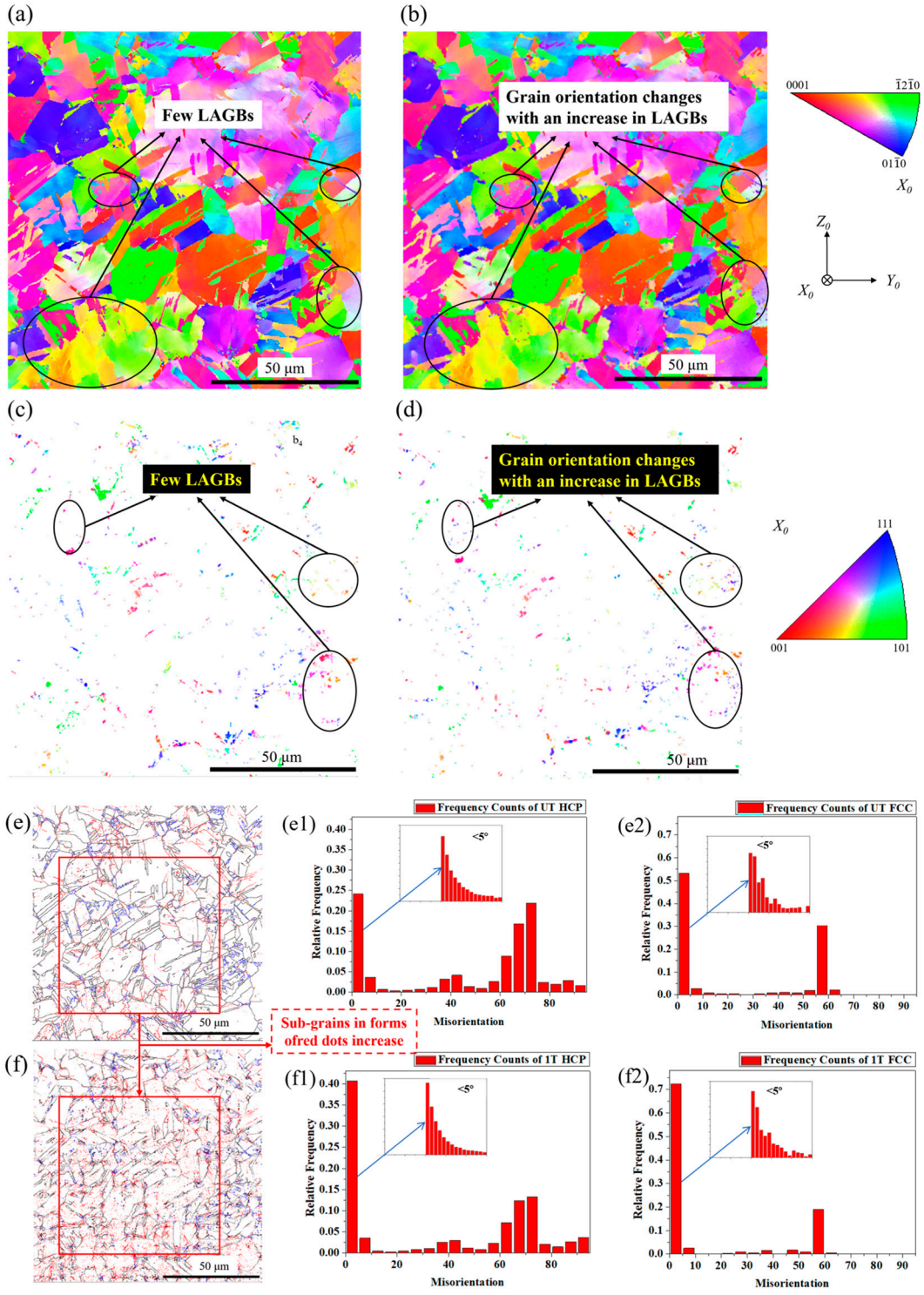


Figure 4. Inverse pole figures (IPFs), grain boundary misorientations and relative frequencies (**e1**,**e2**,**f1**,**f2**) of bulk cobalt. (**a**) HCP-UT, (**b**) HCP-1T, (**c**) FCC-UT, (**d**) FCC-1T, (**e**) UT, (**f**) 1T.

3.3. Defects Change

Kernel average misorientation (KAM) from EBSD is shown in Figure 5a,b and was used to determine misorientations and defects within the Co [18]. In the figure, grains without orientation differences are denoted by blue areas while misorientations and defects are shown by green lines. It is clear that the imposition of the pulsed field promoted the formation of defects and misorientations, and the increase in defect density is seen as one of the main strengthening mechanisms for the enhanced mechanical properties of Co [19].

To further analyze the change of defects, TEM images of the Co are provided in Figure 5c–f. Figure 5c,e show the morphologies of stacking faults and dislocations before the treatment. It is observed that the stacking faults presented multiple parallel stripe-like morphologies, terminating at grain boundaries, and the dislocations show the morphologies of curved entanglements connected to each other as walls. Figure 5d,f show the stacking faults and dislocation regions after PMT. It is evident that a higher density of stacking-fault stripes were formed after the treatment (Figure 5d) and this observation is attributed to the fact that the formation of the stacking faults in Co was facilitated under the pulsed magnetic field due to its high stacking-fault energy [20]. On the other hand, the dislocation multiplied and the dislocation core was extended to form a dislocation net [21] after the treatment (Figure 5f), where many edge dislocations entangled with each other and aggregated to form dislocation walls.

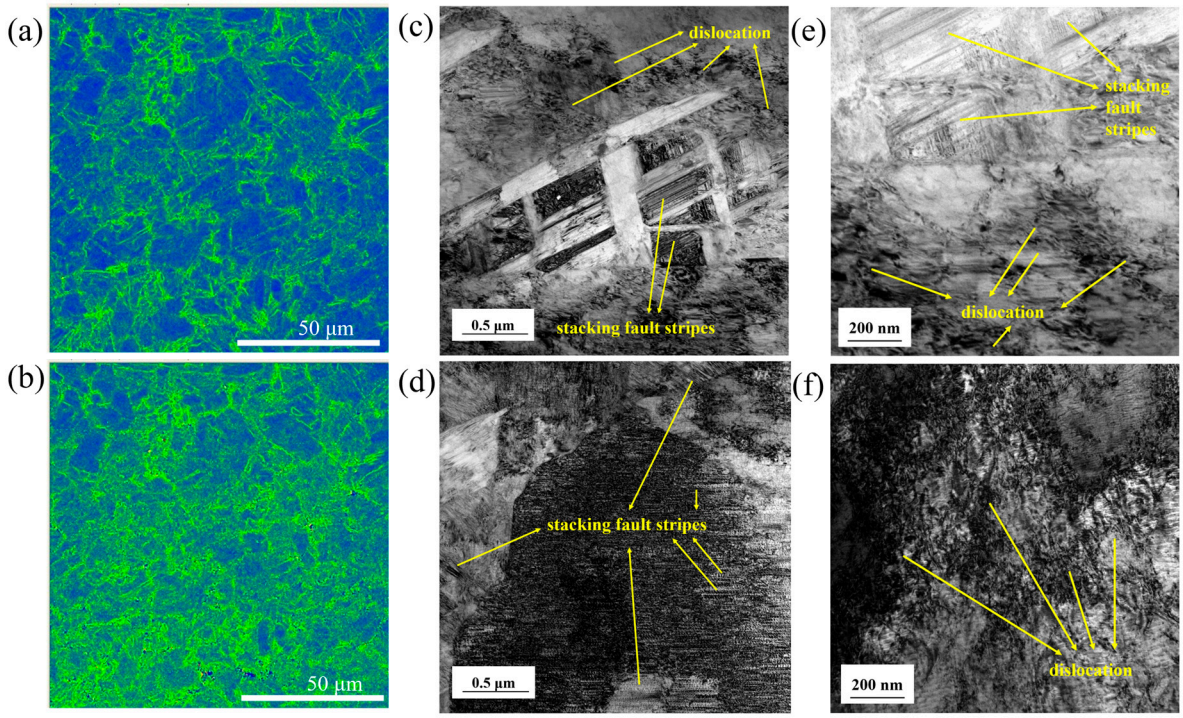


Figure 5. KAM maps of bulk Co and bright-field TEM images. (**a**) UT; (**b**) 1T; (**c**,**e**) UT; (**d**,**f**) 1T.

The formation of these defects is expected to be associated with the phase transformation of Co from FCC to HCP, and Figure 6 gives the TEM observations of the Co phase before and after the treatment to show the structure of the phase. The selected area electron diffraction pattern (SAED) in Figure 6a indicates that the FCC structure without stacking faults was present in the Co while the SAED pattern in the stacking-fault regions in Figure 6c demonstrates the coexistence of HCP and FCC, which follows the Shoji–Nishiyama orientation rule: two-phase close-packed planes being parallel to each other, that is, $(0001)_{HCP}//\{111\}_{FCC}$ [22]. In addition, after PMT, the SAED patterns for the areas both with and without stacking-fault regions in Figure 6d,e indicate the presence of HCP. Based on these observed facts and the results shown in Figure 3 and Table 1, it is expected that phase transformation from FCC to HCP is promoted with an imposition of the pulsed magnetic field, and stacking faults tend to be formed in the HCP phase during the transition. In the atomic layer where the HCP phase and the FCC phase coexisted on the close-packed plane, irregular dislocation lines tended to be formed [23]. With an imposition of the pulsed field, an external energy was introduced to impact these irregular high-energy dislocation lines, and atom migrations within these planes were likely to be facilitated. As a result, the movement of atoms on the close-packed plane was expected to result in

the phase transformation from FCC to HCP; these defects tended to decompose to form incomplete dislocations and stacking faults, and were ultimately retained in the HCP.

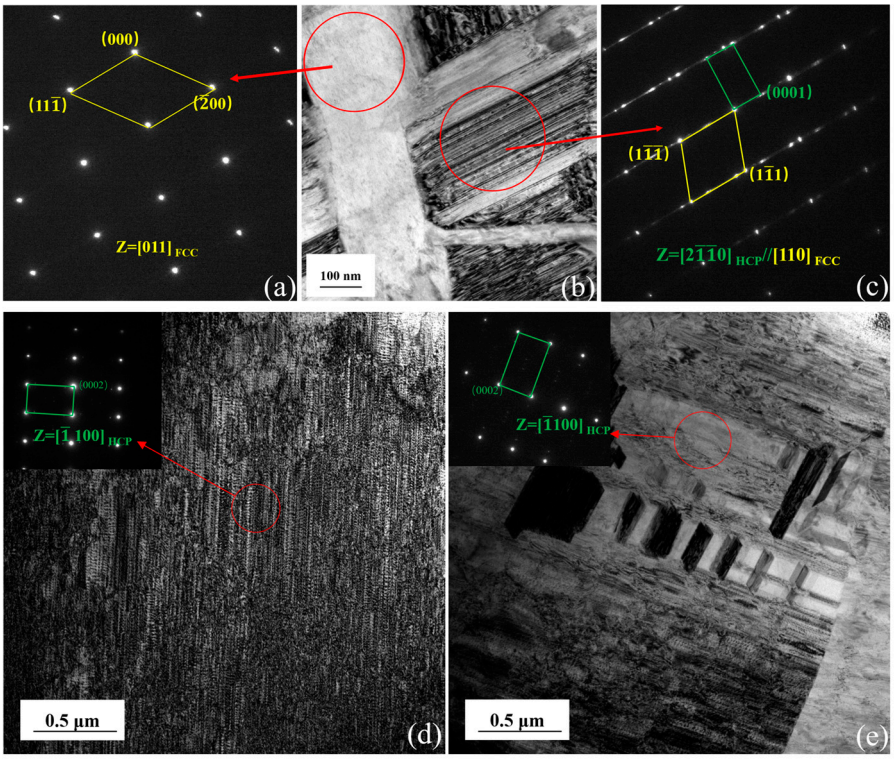


Figure 6. Bright-field TEM images and their corresponding SAED patterns. UT (**a**–**c**); 1T (**d**,**e**).

4. Conclusions

In this study, bulk Co samples were treated by PMT and microstructures were analyzed to correlate with the mechanical performance of the Co. The obtained results indicate that PMT can stimulate the transformation of the high-temperature phase α-Co to the low-temperature phase ε-Co. Misorientations occurred within large grains and led to the formation of sub-grains and LAGBs after the treatment. A significant amount of defects were formed under PMT and enhanced the hardness of the bulk Co. This study shows that as a green, easily operated, and non-destructive post-treatment method, improvement in the performance of the materials can be achieved through PMT by modifying the microstructure, phase distribution, and defects. At present, the diversified application requirements of materials indicate higher requirements for material post-processing technology. For example, in the fields of cutting tools, molds, and aerospace materials, composites of magnetic elements improve the properties of these materials while PMT changes the internal structure and defect distribution of magnetic elements, which can interact with other composite materials and ultimately improve the macroscopic properties of materials. Thus, PMT is a promising post-processing method.

Author Contributions: Conceptualization, Y.L. and J.L.; methodology, Y.L. and J.L.; formal analysis, Y.L.; investigation, Y.L., J.L., H.G., L.Z., Z.C. and L.L.; resources, J.L.; data curation, J.L.; writing—original draft preparation, Y.L.; writing—review and editing, Y.L. and J.L. All authors have read and agreed to the published version of the manuscript.

Funding: The authors wish to acknowledge financial support from the National Nature Science Foundation of China (No. 51975390), the Applied Basic Research Programs of Science and Technology Department of Sichuan Province (No. 2019YJ0110), the Sichuan University and Yibin Municipal People's Government University and City strategic cooperation special fund project (Grant No. 2020CDYB-29), and the Key Research and Development Program of Science and Technology Department of Sichuan Province (No. 2020YFS0575).

Institutional Review Board Statement: Not applicable.

Informed Consent Statement: Not applicable.

Data Availability Statement: Data sharing is not applicable.

Acknowledgments: The authors are grateful to Sichuan University for the equipment support.

Conflicts of Interest: The authors declare no conflict of interest.

References

1. Yin, Y.D.; Rioux, R.M.; Erdonmez, C.K.; Hughes, S.; Somorjai, G.A.; Alivisatos, A.P. Formation of hollow nanocrystals through the nanoscale Kirkendall effect. *Science* **2004**, *304*, 711–714. [CrossRef]
2. Nielsch, K.; Casta, O.F.; Matthias, S.; Lee, W.; Ross, C. Synthesis of Cobalt/Polymer Multilayer Nanotubes. *Adv. Eng. Mater.* **2005**, *7*, 217–221. [CrossRef]
3. Adjam, S.; Mari, D.; Lagrange, T. Strain glass transition of cobalt phase in a cemented carbide. *Int. J. Refract. Met. Hard Mater.* **2019**, *87*, 105161. [CrossRef]
4. Stewart, H.A. Cryogenic treatment of tungsten carbide reduces tool wear when machining medium density fiberboard. *For. Prod. J.* **2004**, *54*, 53–56.
5. Muthuswamy, P.; Dinakaran, D. Evaluation of mechanical and metallurgical properties of cryo-treated tungsten carbide with 25% cobalt. *Mater. Today Proc.* **2020**, *43*, 3463–3469. [CrossRef]
6. Chen, D.; Yao, L.; Chen, Z.H.; Wang, H.P.; Peng, W. Study on Low Cycle Impact Fatigue Performance of WC-Co Cemented Carbides. *Rare Met. Cem. Carbides* **2017**, *45*, 71–75, 80.
7. Quan, S.; Kang, J.; Xing, Z.; Wang, H.; Yanfei, H.; Guozheng, M.; Liu, H. Effect of pulsed magnetic field treatment on the residual stress of 20Cr2Ni4A steel. *J. Magn. Magn. Mater.* **2019**, *476*, 218–224.
8. Shao, Q.; Wang, G.; Wang, H.; Xing, Z.; Cao, Q. Improvement in uniformity of alloy steel by pulsed magnetic field treatment. *Mater. Sci. Eng. A* **2020**, *799*, 140143. [CrossRef]
9. Fei, H.L.; Wu, H.; Yang, X.; Xiong, J.; Liu, J. Pulsed magnetic field treatment of cBN tools for improved cutting performances. *J. Manuf. Process.* **2021**, *69*, 21–32. [CrossRef]
10. Ma, L.; Zhao, W.; Liang, Z.; Wang, X.; Xie, L.; Jiao, L.; Zhou, T. An investigation on the mechanical property changing mechanism of high speed steel by pulsed magnetic treatment. *Mater. Sci. Eng. A* **2014**, *609*, 16–25. [CrossRef]
11. Tang, G.; Xu, Z.; Miao, T.; Chen, X.; Zhou, H.; Lu, A. Effect of a pulsed magnetic treatment on the dislocation substructure of a commercial high strength steel. *Mater. Sci. Eng. A* **2005**, *398*, 108–112. [CrossRef]
12. Li, G.R.; Li, Y.M.; Wang, F.F.; Wang, H.M. Microstructure and performance of solid TC4 titanium alloy subjected to the high pulsed magnetic field treatment. *J. Alloys Compd.* **2015**, *644*, 750–756. [CrossRef]
13. Liu, J.; Wei, C.; Yang, G.; Wang, L.; Wang, L.; Wu, X.; Jiang, K.; Yang, Y. A Novel Combined Electromagnetic Treatment on Cemented Carbides for Improved Milling and Mechanical Performances. *Metall. Mater. Trans. A* **2018**, *49*, 4798–4808. [CrossRef]
14. Huang, J.Y.; Wu, Y.K.; Ye, H.Q. Phase transformation of cobalt induced by ball milling. *Appl. Phys. Lett.* **1995**, *66*, 308. [CrossRef]
15. Cai, Y.; Zhu, L.; Cui, Y.; Shan, M.; Han, J. Fracture and wear mechanisms of FeMnCrNiCo + x(TiC) composite high-entropy alloy cladding layers. *Appl. Surf. Sci.* **2020**, *543*, 148794. [CrossRef]
16. Glez, J.C.; Driver, J. Orientation distribution analysis in deformed grains. *J. Appl. Crystallogr.* **2001**, *34*, 280–288. [CrossRef]
17. Kostka, A.; Tak, K.G.; Hellmig, R.J.; Estrin, Y.; Eggeler, G. On the contribution of carbides and micrograin boundaries to the creep strength of tempered martensite ferritic steels. *Acta Mater.* **2007**, *55*, 539–550. [CrossRef]
18. Calcagnotto, M.; Ponge, D.; Demir, E.; Raabe, D. Orientation gradients and geometrically necessary dislocations in ultrafine grained dual-phase steels studied by 2D and 3D EBSD. *Mater. Sci. Eng. A* **2010**, *527*, 2738–2746. [CrossRef]
19. Wang, C.; Shen, X.J.; An, Z.B.; Zhou, L.C.; Chai, Y. Effects of laser shock processing on microstructure and mechanical properties of K403 nickel-alloy. *Mater. Des.* **2016**, *89*, 582–588. [CrossRef]
20. Zhang, L.; Hu, Z.; Zhang, L.; Wang, H.; Li, J.; Li, Z.; Yu, J.; Wu, B. Enhancing the strength-ductility trade-off in a NiCoCr-based medium-entropy alloy with the synergetic effect of ultra fine precipitates, stacking faults, dislocation locks and twins. *Scr. Mater.* **2022**, *211*, 114497. [CrossRef]
21. Liu, X.Y.; Capolungo, L.; Hunter, A. Screw dislocation impingement and slip transfer at fcc-bcc semicoherent interfaces. *Scr. Mater.* **2021**, *201*, 113977. [CrossRef]
22. Liu, W.; An, X.; Jiang, W.; Ni, S.; Song, M. Microstructural evolution of a polycrystalline cobalt during tensile deformation. *Mater. Sci. Eng. A.* **2021**, *826*, 141970. [CrossRef]
23. Ma, R.B.; Zhou, L.L.; Liang, Y.C.; Chen, Q.; Tian, Z.; Liu, R.S.; Mo, Y.F.; Gao, T.H.; Xie, Q. The effect of HCP on the formation of twin boundaries and dislocations in Ni–Co alloys. *Curr. Appl. Phys.* **2021**, *29*, 18–23. [CrossRef]